

Reviewer #1)

### **General comments**

This manuscript presents a valuable three-year dataset (2020-2022) exploring how heavy precipitation and the resulting YRDW influence microbial carbon dynamics in the nECS. The authors integrate satellite-based salinity, PP, HPP, and FDOM measurements with nutrient-addition bioassays. The topic is timely and relevant to Biogeosciences, addressing the interaction between hydrological forcing and microbial processes in marginal seas.

The manuscript is well organized and clearly written, and the field observations are impressive in scope. However, several aspects of the analysis and interpretation require further clarification before the conclusions can be fully supported. In particular, the paper tends to extend beyond the range of the presented evidence, and the causal links between precipitation, DOM quality, and microbial carbon partitioning are not fully demonstrated.

### **[Response]**

Thank you very much for your positive and valuable comments that have greatly improved the quality of the revised manuscript. We have incorporated your comments and suggestions into the revised version as much as we can.

I outline below the main points that, in my view, require attention:

**Comment #1)** The paper draws a direct causal chain from precipitation and YRDW variability to microbial carbon partitioning and trophic balance. While the correlation between hydrological forcing and microbial parameters is evident, the discussion extrapolates local observational patterns to ecosystem-scale mechanisms (e.g., "enhanced microbial loop and reduced food-web efficiency") without direct process measurements of carbon transfer (e.g., respiration or bacterial growth efficiency).

The authors are encouraged to clarify which interpretations are empirically supported and which remain conceptual or inferential. This distinction will help strengthen the credibility of the conclusions.

### **[Response]**

Thank you for this critical comment. Our combined response to your Comments #1 is provided, along with the response to your Comment #2 below.

**(Comment #2).** The use of the HPP:PP ratio as an indicator of microbial loop intensity is informative but limited. Without concurrent measurements of respiration or BGE, this ratio reflects only relative production rates rather than the efficiency of carbon transfer or sequestration. The authors briefly acknowledge this point in the manuscript, but a more explicit discussion in the main text would strengthen the interpretation and clarify the limitations of using HPP:PP as a mechanistic indicator.

**[Response to comments #1 and #2]**

Thank you for this valuable comment. We fully agree with your point that respiration (or bacterial carbon demand) data is essential for discussing carbon flow through the microbial loop—that refers to the role of microbial loop in biogeochemical carbon cycling. As you know, microbial loop has two components: the trophic link and the sink of photosynthetically fixed carbon (i.e., respiration). Respiration data should therefore be included to evaluate the role of the microbial loop in the biogeochemical carbon cycle, as it provides direct information on carbon flow via microbial loop.

Although we measured respiration, we reserved these results for a forthcoming paper that addresses the metabolic balance (heterotrophic vs. autotrophic) in the northern East China Sea (Fig. R1 below). As shown in Fig. R1, heterotrophic prokaryotic respiration (HPR) increased in August 2020, resulting in the highest heterotrophic prokaryotic carbon demand (HPCD = HPP + HPR) under the strongest influence of YRDW. This suggests that HP mineralized a large amount of DOC supplied via YRDW. The elevated HPCD indicates an intensified microbial loop, while the low growth efficiency (HPGE) suggests that refractory DOC dominance and phosphorus deficiency shifted microbial carbon partitioning toward respiration rather than production. By contrast, the HPP:PP ratio provides insight into the role of the microbial loop in microbial food web processes. Since respiration data were not included in this manuscript, we have constrained our discussion, based on your comments, to “the role of the microbial loop in microbial food-web processes.” Accordingly, the manuscript has been revised as follows:

Line 28: enhanced carbon flow via **microbial loop**

→ enhanced carbon flow via **microbial food web**

Line 89: (1) to interpret the role of microbial loop in microbial food web process and **biogeochemical carbon cycles,**

→ (1) to interpret the role of microbial loop in microbial food web process  
~~biogeochemical carbon cycles,~~

Line 378: 4.4 Impacts of YRDW in intensifying microbial loop

→ 4.4 Impacts of YRDW in intensifying microbial food web

Line 382: To evaluate the carbon flow through the microbial loop,

→ To evaluate the carbon flow through the microbial food web,

Line 386: supporting a comparable amount of carbon flow through the microbial loop (Rowe et al., 2025).

→ supporting a comparable amount of carbon flow through the microbial food web  
(Rowe et al., 2025)

After discussion among co-authors, we decided that addressing respiration would be more appropriate in the forthcoming paper, which focuses on the role of microbial loop as an “organic carbon sink”. We sincerely hope this response is acceptable.

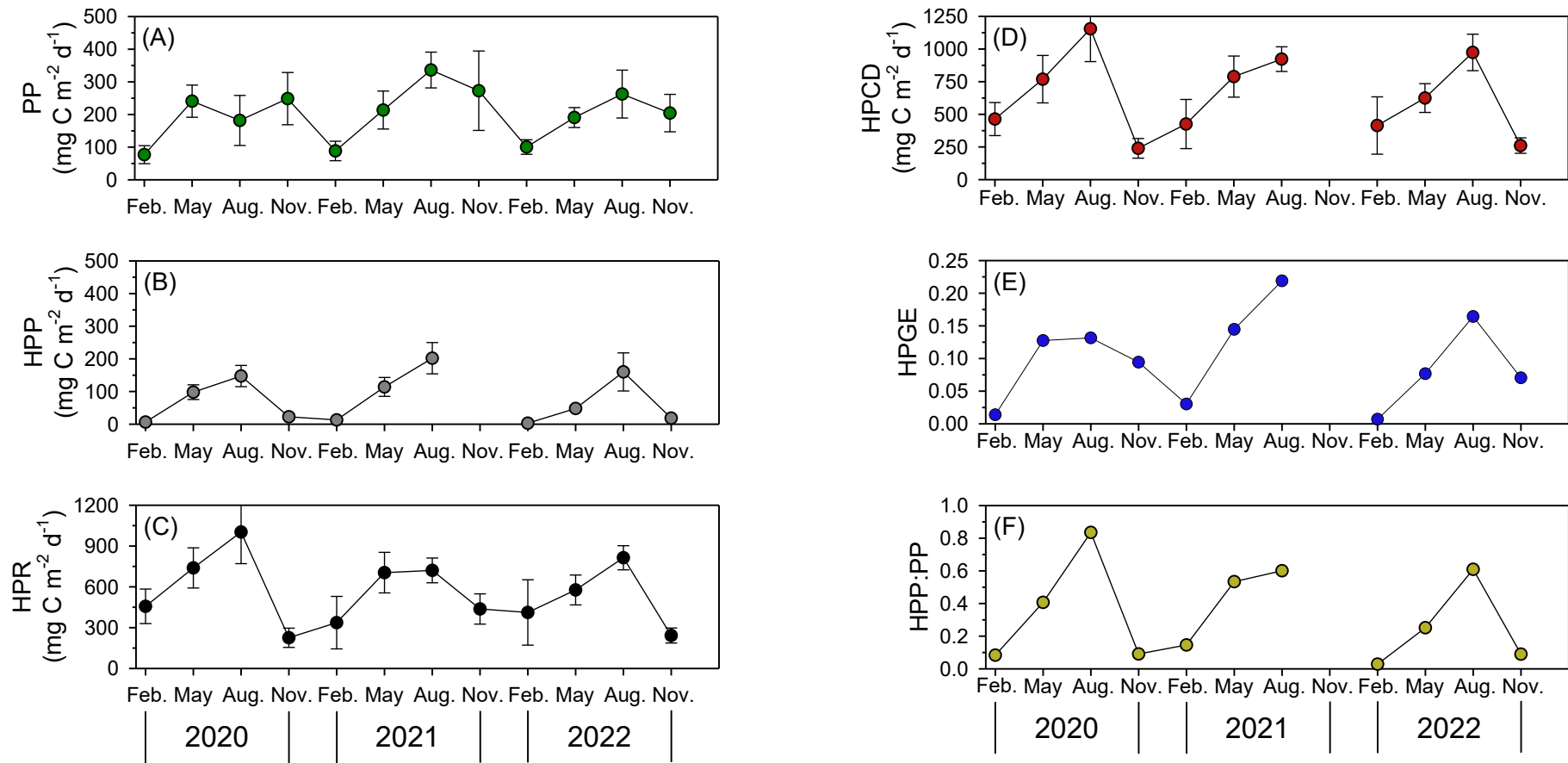


Figure R1. Seasonal variation of primary production (PP) (A), heterotrophic prokaryotes production (HPP) (B), heterotrophic prokaryotes respiration (HPR) (C), heterotrophic prokaryotes carbon demand (HPCD) (D), heterotrophic prokaryotes growth efficiency (HPGE) (E), heterotrophic prokaryotes production to primary production (HPP:PP) (F) in the northern East China Sea. PP, HPP, and HPR are integrated within the euphotic depth. Error bars represent standard errors.

**(Comment #3)** The manuscript would benefit from a better balance between the Results and Discussion sections. The results are presented rather succinctly, whereas the discussion is extensive and mechanism-oriented. Presenting slightly more quantitative detail in the Results—especially regarding interannual trends and variability—would make the argumentation in the Discussion easier to follow and more persuasive.

### **[Response to comment #3]**

Thank you for your suggestion regarding the balance between the Results and Discussion sections. Following your comment, we have added a new figure (Figure 3) showing detailed vertical profiles of temperature, salinity, DOC, chlorophyll-a, prokaryote abundance (PA), and heterotrophic prokaryotes production (HPP) in revised manuscript to provide clearer quantitative context for the seasonal and interannual variability. We have also revised the Results section to more explicitly describe these vertical patterns and their seasonal contrasts in line 187-235 in the manuscript, as detailed below.

### 3.1 Hydrographic conditions

Based on Temperature-Salinity (T-S) diagrams, the current systems in the study area were defined by 2-4 water masses that vary seasonally (Fig. 2). The two main currents appearing in the nECS are the Kuroshio Source Water (KSW) and the Shelf Mixed Water (SMW) (Fig. 2). The KSW is formed by the convergence of the TWC and the TWW, which are both branches of the main Kuroshio Current in the nECS and are characterized by high temperature and salinity (Supplement Fig. S1). In contrast, the SMW is formed by the mixing of the KSW with the Chinese Coastal Current (CC). The CC, which is mainly observed on the shelf side of the East China Sea, is characterized by cold and low-salinity properties (Li et al., 2006). As a result, the SMW exhibits relatively lower temperature and salinity due to the influence of the CC. During February (winter), May (spring), and November (autumn), the nECS consisted of KSW and SMW (Fig. 2A, B, D, E, F, H, I, J, L; Table S1). However, during August (summer), a more complex water mass distribution was observed due to strong stratification and substantial freshwater input: TWC and YRDW were present near the surface, whereas TWW and SMW were observed in the mid to lower layers, which differed from other seasons (Fig. 2C, G, K; Table S1). The satellite images of sea surface salinity (Fig. 1), together with the T-S diagrams (Fig. 2), clearly revealed that YRDW (< 31 psu, the blue-

green colors in Fig. 1C, G, K) originating from the Yangtze River in August expands northeastward to the nECS located approximately 300 km away from the Yangtze River estuary. The expansion of YRDW to the nECS was greatest in August 2020, followed by August 2022 and 2021, respectively (Fig. 1; Fig. 2).

### 3.2 DOC, Chl-*a* and primary production

The vertical distributions of DOC reflected seasonal changes in water column structure (Fig. 3). In February and November, DOC concentrations were relatively homogeneous within the MLD (50–70 m), averaging  $65 \pm 2 \mu\text{M}$  (53 – 76  $\mu\text{M}$ ) and  $64 \pm 2 \mu\text{M}$  (55 – 83  $\mu\text{M}$ ), respectively (Fig. 3C, W). In contrast, during May and August, DOC concentrations increased with decreasing MLD, averaging  $72 \pm 1 \mu\text{M}$  (66 – 74  $\mu\text{M}$ ) in May and  $86 \pm 3 \mu\text{M}$  (75 – 130  $\mu\text{M}$ ) in August (Fig. 3K, Q; Table 1).

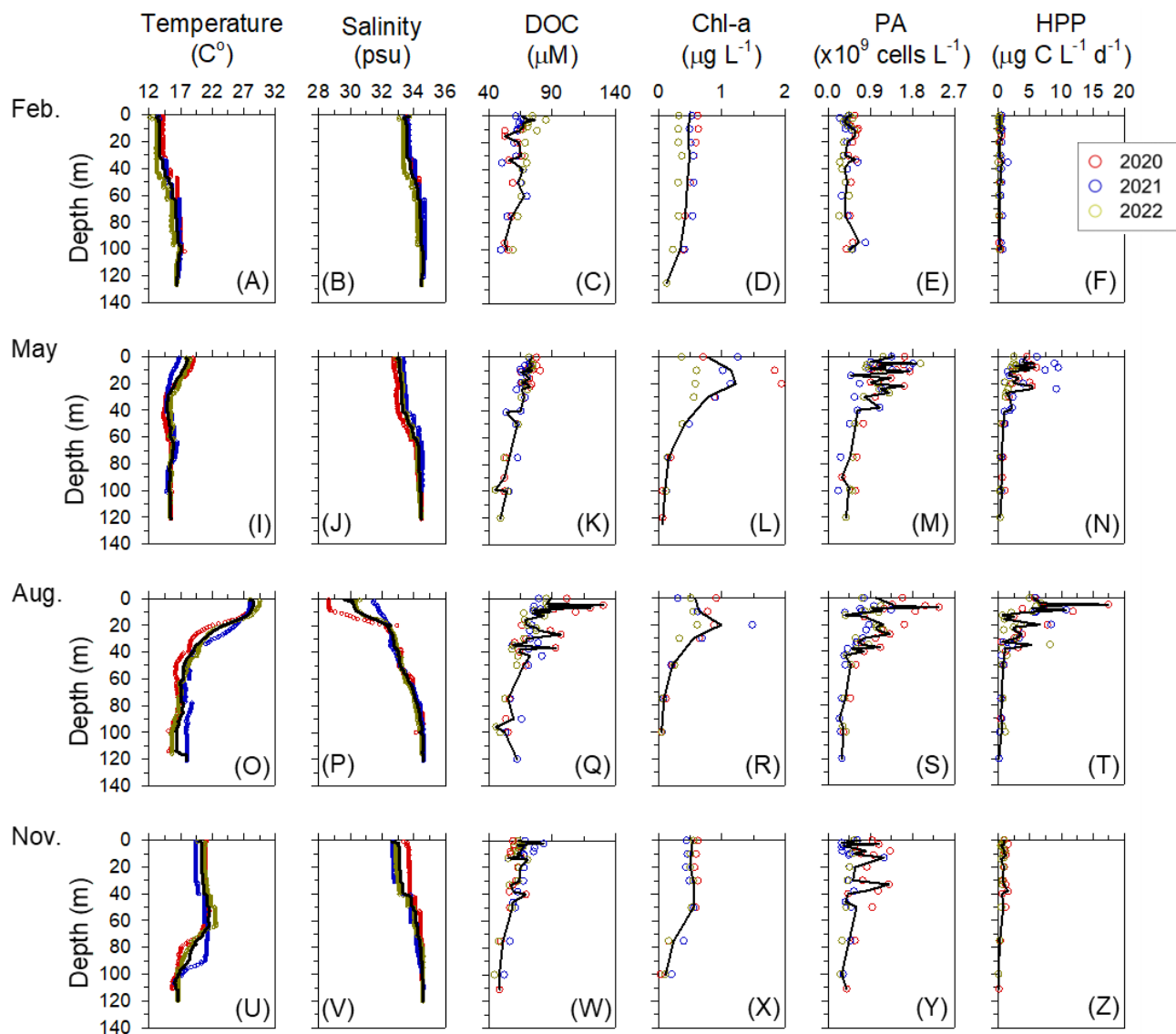
Elevated DOC concentrations were particularly evident in August within the low-salinity surface layer (upper 10 m), where values averaged  $95 \pm 19 \mu\text{M}$  (76–130  $\mu\text{M}$ ; Fig. 3P, Q). Among the summer observations, August 2020 exhibited the highest DOC concentrations ( $104 \pm 5 \mu\text{M}$ ), which were significantly higher than those in August 2021 and 2022 ( $77 \pm 1 \mu\text{M}$  and  $80 \pm 3 \mu\text{M}$ , respectively;  $p = 0.002$ ), coinciding with the strongest influence of YRDW observed during the study period (Fig. 1C, 4A).

Chl-*a* concentrations within the MLD followed a similar pattern: homogeneously low in February ( $0.47 \pm 0.02 \mu\text{g L}^{-1}$ ;  $0.42 - 0.49 \mu\text{g L}^{-1}$ ), increasing in May ( $1.05 \pm 0.24 \mu\text{g L}^{-1}$ ;  $0.77 - 1.22 \mu\text{g L}^{-1}$ ) with the development of thermal stratification, remaining elevated in August (avg.  $0.74 \pm 0.22 \mu\text{g L}^{-1}$ ;  $0.58 - 0.99 \mu\text{g L}^{-1}$ ) under strong haline stratification associated with YRDW intrusion, and decreased in November (avg.  $0.53 \pm 0.02 \mu\text{g L}^{-1}$ ;  $0.50 - 0.55 \mu\text{g L}^{-1}$ ) (Fig. 3I, P, L, R).

PP, integrated over the euphotic depth, followed a similar seasonal pattern, increasing from May to August and peaking at  $336 \pm 55 \text{ mg C m}^{-2} \text{ d}^{-1}$  (August 2021) and  $263 \pm 73 \text{ mg C m}^{-2} \text{ d}^{-1}$  (August 2022) (Fig. 4D). Notably, PP in August 2020 ( $182 \pm 77 \text{ mg C m}^{-2} \text{ d}^{-1}$ ) was significantly lower than other years ( $p = 0.028$ ) (Fig. 4D), despite high YRDW input.

### 3.3 Prokaryotes abundance and heterotrophic prokaryotes production

Mean PA within the euphotic depth was lowest and vertically homogeneous in February ( $0.46 \pm 0.03 \times 10^9$  cells L<sup>-1</sup>;  $0.35 - 0.59 \times 10^9$  cells L<sup>-1</sup>). In contrast, PA reached its highest values in May ( $1.28 \pm 0.09 \times 10^9$  cells L<sup>-1</sup>;  $0.48 - 1.88 \times 10^9$  cells L<sup>-1</sup>), before declining in August ( $0.99 \pm 0.09 \times 10^9$  cells L<sup>-1</sup>;  $0.37 - 2.36 \times 10^9$  cells L<sup>-1</sup>) and November ( $0.66 \pm 0.08 \times 10^9$  cells L<sup>-1</sup>;  $0.28 - 1.29 \times 10^9$  cells L<sup>-1</sup>) (Fig. 3; Table 1). PA correlated positively with DOC ( $\rho = 0.255$ ,  $p < 0.001$ ) and Chl-*a* ( $\rho = 0.281$ ,  $p < 0.001$ ). HPP within the euphotic depth followed a seasonal cycle: lowest in February ( $0.33 \pm 0.12 \mu\text{g C L}^{-1} \text{ d}^{-1}$ ;  $0.20 - 0.58 \mu\text{g C L}^{-1} \text{ d}^{-1}$ ), rising in May ( $3.73 \pm 1.37 \mu\text{g C L}^{-1} \text{ d}^{-1}$ ;  $1.76 - 5.86 \mu\text{g C L}^{-1} \text{ d}^{-1}$ ), reaching a consistent summer peak in August ( $5.51 \pm 4.08 \mu\text{g C L}^{-1} \text{ d}^{-1}$ ;  $0.69 - 17.43 \mu\text{g C L}^{-1} \text{ d}^{-1}$ ), and then declining in November ( $0.83 \pm 0.26 \mu\text{g C L}^{-1} \text{ d}^{-1}$ ;  $0.43 - 1.24 \mu\text{g C L}^{-1} \text{ d}^{-1}$ ) (Fig. 3). HPP correlated positively with temperature ( $\rho = 0.525$ ,  $p < 0.001$ ), DOC ( $\rho = 0.457$ ,  $p < 0.001$ ) and Chl-*a* ( $\rho = 0.398$ ,  $p < 0.001$ ) consistent with the observed summer peak.



70 **Figure 3.** Vertical profiles of temperature, salinity, dissolved organic carbon (DOC), chlorophyll-a (Chl-a), heterotrophic prokaryote abundance (PA), and heterotrophic prokaryote production (HPP) in the northern East China Sea from 2020 to 2022. Each symbol represents the average value at a given depth from 7–8 stations sampled during each survey, and the solid black line denotes the mean of the three-year averages.

**Table S1. Seasonal temperature and salinity ranges used to define major water masses in the northern East China Sea in this study. KSW: Kuroshio source water, SMW: Shelf mixed water, YRDW: Yangtze river diluted water, TWW: Tsushima warm water, TWC: Taiwan warm current.**

	Seasonal temperature (°C) and salinity (psu) range				
	KSW	SMW	YRDW	TWW	TWC
Winter	8.4 < T < 24.5	8.8 < T < 15			
	33.6 < S < 35.2	32.4 < S < 33.6			
Spring	11.5 < T < 29.4	12 < T < 21			
	33.5 < S < 35.2	31.2 < S < 33.5			
Summer		14 < T < 23	23 < T	14 < T	23 < T
		31 < S < 34	S < 31	34 < S	31 < S < 34.2
Autumn	11.8 < T < 27.3	14.3 < T < 24.2			
	33.4 < S < 34.9	31.9 < S < 33.4			

75

**Comment #4)** The study attributes seasonal variability of HPP mainly to precipitation and phosphorus limitation. However, temperature, grazing pressure, or water-column stability may also influence microbial activity. A brief discussion acknowledging these potential co-drivers would provide a more balanced interpretation.

80 **[Response to comment #4]**

Thank you for this insightful comment. We agree that temperature, grazing pressure, and water-column stability are important co-drivers influencing microbial activity. Indeed, temperature stimulates bacterial metabolism, as confirmed by the significant correlation between HPP and temperature ( $p < 0.001$ , Table R1, *Dataset\_Water\_column.csv*). However, the observed 3– to 300-fold increases in HPP across the seasonal temperature gradient substantially exceed the expected  $Q_{10}$  relationship (~2-fold increase per 10°C). This indicates that other parameters covarying with temperature likely exert the dominant control on HPP (Hyun and Kim, 2003; Kirchman et al., 2009; Hyun et al., 2016).

85

90 **Table. R1 Spearman's rank correlation coefficients ( $\rho$ ) between heterotrophic prokaryotes parameters (production, HPP; abundance, PA) and temperature, chlorophyll *a* (Chl-*a*), and dissolved organic carbon (DOC) pooled over three years in the northern East China Sea.**

Parameter	HPP	PA
Temperature	$\rho = 0.525$ ( $p < 0.001$ )	$\rho = 0.364$ ( $p < 0.001$ )
Chl- <i>a</i>	$\rho = 0.398$ ( $p < 0.001$ )	$\rho = 0.281$ ( $p < 0.001$ )
DOC	$\rho = 0.457$ ( $p < 0.001$ )	$\rho = 0.255$ ( $p < 0.001$ )

Furthermore, despite high HPP observed during summer, the concurrent decrease prokaryotes abundance (PA) suggests that strong top-down control, such as grazing pressure, may have been important during this period (Fig. 4C, E; Chiang et al., 2003; Tsai et al., 2013). Nevertheless, as the main focus of this study was on bottom-up controls on HPP associated with YRDW influence and grazing pressure by protists was not directly measured, we did not attempt a quantitative assessment of top-down control. I hope future research can further investigate these processes.

100 Water-column stability refers to the degree of vertical stratification that constrains vertical mixing and regulates the residence time and vertical distribution of substrates and microbial communities. To account for this physical structure, parameters used to interpret HPP were evaluated within depth ranges appropriate for their underlying processes across all seasons. Specifically, DOC was evaluated as average values within the mixed layer depth (MLD), where stratification affects substrate accumulation, whereas primary production (PP) and Chl-*a* were evaluated within the euphotic zone, where photosynthetic activity occurs.

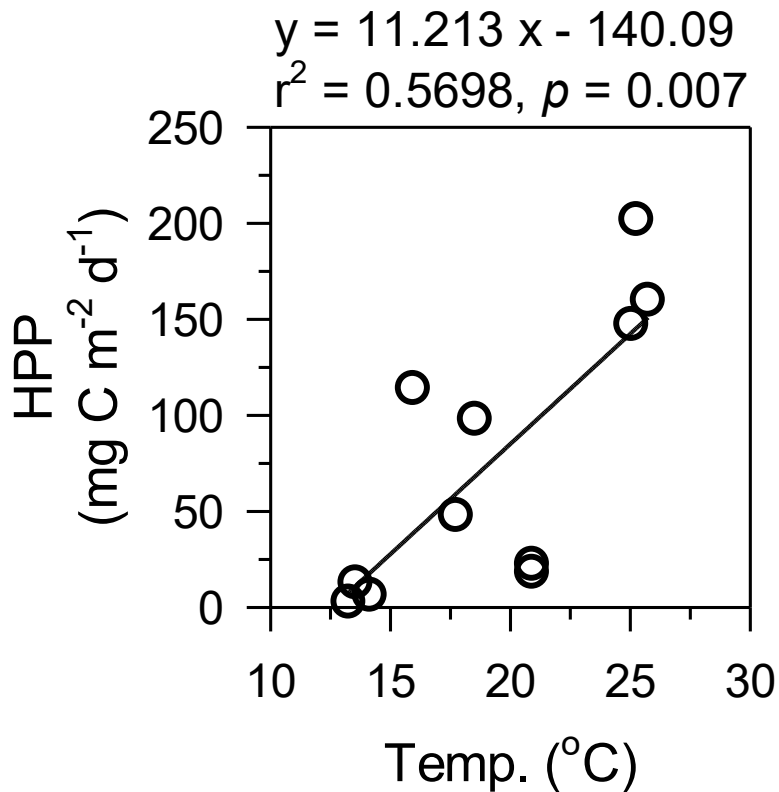
105 Consequently, in response to your comment, we have added the following paragraphs at **Lines 231 and 238 in revised manuscript:**

110 Line 231 in revised manuscript:

HPP within the euphotic depth followed a seasonal cycle: lowest in February ( $0.33 \pm 0.12 \mu\text{g C L}^{-1} \text{d}^{-1}$ ;  $0.20 - 0.58 \mu\text{g C L}^{-1} \text{d}^{-1}$ ), rising in May ( $3.73 \pm 1.37 \mu\text{g C L}^{-1} \text{d}^{-1}$ ;  $1.76 - 5.86 \mu\text{g C L}^{-1} \text{d}^{-1}$ ), reaching a consistent summer peak in August ( $5.51 \pm 4.08 \mu\text{g C L}^{-1} \text{d}^{-1}$ ;  $0.69 - 17.43 \mu\text{g C L}^{-1} \text{d}^{-1}$ ), and then declining in November ( $0.83 \pm 0.26 \mu\text{g C L}^{-1} \text{d}^{-1}$ ;  $0.43 - 1.24 \mu\text{g C L}^{-1} \text{d}^{-1}$ ) (Fig. 3). HPP correlated positively with  
115 temperature ( $\rho = 0.525$ ,  $p < 0.001$ ), DOC ( $\rho = 0.457$ ,  $p < 0.001$ ) and Chl-*a* ( $\rho = 0.398$ ,  $p < 0.001$ ), consistent with the observed summer peak.

Line 238 in revised manuscript:

In the present study, one of the most prominent features observed in oceanographic and  
120 microbiological properties was the consistent summer peak in HPP (Fig. 4E). Considering the typically enhanced HPP coupled with phytoplankton bloom in spring in the middle latitudes of the northern hemisphere (Amon and Benner, 1998; Lemée et al., 2002; Gomes et al., 2015), our results showing consistently high summer peaks in microbiological parameters are noteworthy. Plankton activities are positively correlated with temperature in many marine systems, a pattern that has been widely reported  
125 in previous studies (White et al., 1991; Robinson and Williams, 1993), suggesting that elevated summer temperatures may partially contribute to high HPP. However, assuming a  $Q_{10}$  of 2, a  $10 \text{ }^\circ\text{C}$  temperature increase from  $15 \text{ }^\circ\text{C}$  to  $25 \text{ }^\circ\text{C}$  would yield an approximately twofold increase in HPP. In contrast, estimates from the observed seasonal temperature–HPP relationship suggest a fivefold increase from 28 to  $140 \text{ mg C m}^{-2} \text{ d}^{-1}$  (Supplement Fig. S3), exceeding that expectation. In addition to temperature, positive  
130 correlations of HPP DOC ( $\rho = 0.457$ ,  $p < 0.001$ ) and Chl-*a* ( $\rho = 0.398$ ,  $p < 0.001$ ) indicate that these factors acted as co-drivers of the consistently elevated HPP observed in summer, coinciding with the expansion of YRDW (Fig. 1; Table 1).



135 Figure S3. Relationship between the average temperature within the euphotic zone and heterotrophic prokaryotes production (HPP) integrated over the euphotic zone in the northern East China Sea, using seasonally averaged values from 2020 to 2022.

140 **Comment #5)** The nutrient-limitation bioassay (Fig. 7) is compelling; however, the differences between 12-h and 26.5-h incubations could affect comparability. Please discuss potential bias due to unequal incubation times.

**[Response to comment #5]**

145 Thank you for the positive feedback on the nutrient-limitation bioassay. Regarding incubation time, we note that our interpretation focuses on HPP differences between treatments and the unamended control, thereby minimizing possible bias arising from the small variation in incubation duration. Incubation periods typically ranging from 12 to 24 h have been widely adopted in previous studies (Hyun, 2006; Rahav et al., 2018; Kim et al., 2025).

We revised our manuscript as follows:

**[Revision]**

150 Line 178: Subsamples for measuring HPP in triplicate were taken after 12 hours of incubation in August 2020 and after 26.5 hours in April 2021.

→ Subsamples for measuring HPP were collected in triplicate after 12 h incubation in August 2020 and 26.5 h in April 2021. The longer incubation time in April 2021 was chosen to account for lower spring temperatures that could delay microbial metabolic responses (Table 2).

155

Minor comments

#1) It would be helpful to clarify whether HPP and PP were measured concurrently at the same sampling stations. If not, a short note on how this may affect the interpretation of HPP:PP ratios would be valuable.

160 **[Response]**

Thank you for this comment. HPP and PP were measured concurrently at the same stations. PP samples were collected across light penetration depths (100%, 50%, 30%, 12%, 5%, 1% of surface irradiance), while HPP was measured at the 100% , 30% and 1% light depths. We have revised the manuscript to clarify this sampling design as follows:

165

**[Revision]**

Line 115: Seawater samples for chemical and biological analyses were collected at designated water 115 depths of 0, 10, 20, 30, 50, 75, 100, 120 meters, as well as at the 1% light penetration depth.

→ Seawater samples for chemical and biological analyses were collected concurrently at the same 170 sampling stations. Sampling was conducted at standard depth (0, 10, 20, 30, 50, 75, 100, and 120 m). Samples for measuring PP were collected at depths corresponding to 30% and 1% of surface photosynthetically active radiation (PAR), determined from Secchi disk measurements. The 1% light depth was defined as the euphotic depth (see *Dataset\_Water\_column.csv*). This sampling design enabled direct comparison of HPP and PP.

175

#2) The authors might consider adding a simple schematic summarizing how YRDW affects nutrient stoichiometry, DOM composition, and microbial carbon flow.

**[Response]**

180 Thank you for this suggestion. A conceptual schematic integrating YRDW effects on nutrient stoichiometry, DOM composition, and microbial carbon flow (including respiratory processes) is under development for a forthcoming study on the fate of carbon in microbial loop. As the present manuscript focuses solely on production-based observations without respiration measurements, we have chosen not to include such a schematic here in order to maintain consistency with the scope of the study.

185 #3) In the Conclusion, tone down generalizations such as “greatly regulates” or “strongly enhances”.

**[Response]**

Thank you for this constructive comment. We revised the Conclusion to tone down generalizations and to better align the wording more closely with the supporting evidence. The specific revisions are as follows:

190

**[Revision]**

Line 411: we present that the YRDW greatly alters the concentrations and bioavailability of DOC and nutrient regimes,

195 → we **demonstrate** that the YRDW **substantially** alters the concentrations and bioavailability of DOC and nutrient regimes,

Line 411: In general, the YRDW was primarily responsible for the enhanced HPP in the nECS in summer by supplying DOC and stimulating high phytoplankton biomass (Fig. 4D, 5A).

200 → In general, the YRDW was **a major contributor to elevated** HPP in the nECS **during** summer by supplying DOC and stimulating high phytoplankton biomass (Fig. 5D, 6A).

Line 426: These results are also applicable to other ocean basins that receive large terrestrial DOM inputs, and are experiencing climate warming along with increased precipitation and riverine inputs (e.g., Amazon River and Arctic Ocean).

→ These results may also be relevant in other ocean basins that receive large terrestrial DOM inputs, and are experiencing climate warming along with increased precipitation and riverine inputs (e.g., Amazon River and Arctic Ocean).

205

#4) The use of 0.2  $\mu\text{m}$  filtration followed by a 9:1 mixture of filtered and unfiltered seawater seems appropriate for reducing grazing while preserving the original bacterial assemblage. Still, the rationale could be clarified briefly in the Methods to help readers understand the intention behind this experimental set up.

210

#### [Response]

Thank you for this helpful comment. We have clarified the rationale for the filtration and mixing approach in Methods section as follows:

215

#### [Revision]

Line 173: Sea water samples were collected at a depth of 10 m at each site, and filtered through polycarbonate filter (0.2  $\mu\text{m}$  pore size) to remove protozoan grazers. The filtered water was mixed with unfiltered sea water in polycarbonate (PC) bottles at 9:1 ratio, and then dispensed into one liter PC bottles.

220

→ Seawater samples were collected at a depth of 10 m at each site, and filtered through polycarbonate filter (0.2  $\mu\text{m}$  pore size) to remove protozoan grazers (Kim et al., 2025). The filtered water was mixed with unfiltered seawater at a 9:1 ratio in one liter polycarbonate bottles to minimize bottle effects while maintaining the natural bacterial assemblage (Ferguson et al., 1984).

225

230

## Technical corrections

The panel labels (A–L) in Figure 1 seem unnecessary, as they are not mentioned in the main text. Consider removing them or clarifying their meaning in the caption.

### **[Response]**

235 We appreciate the reviewer's comment. The panel labels (A–L) in Fig. 1 are explicitly referred to in the text (Lines 199, 211, and 287 in original manuscript) when specific seasonal patterns are discussed.

240

245

250

255

## Reference

260

Cao, S., Sun, F., Lu, D., and Zhou, Y.: Characterization of the refractory dissolved organic matter (rDOM) in sludge alkaline fermentation liquid driven denitrification: effect of HRT on their fate and transformation, *Water Res.*, 159, 135–144, <https://doi.org/10.1016/j.watres.2019.04.063>, 2019.

Chiang, K.-P., Lin, C.-Y., Lee, C.-H., Shiah, F.-K., and Chang, J.: The coupling of oligotrich ciliate  
265 populations and hydrography in the East China Sea: spatial and temporal variations, *Deep-Sea Res. II*, 50, 1279–1293, [https://doi.org/10.1016/S0967-0645\(03\)00062-9](https://doi.org/10.1016/S0967-0645(03)00062-9), 2003.

Ferguson, R. L., Buckley, E. N., and Palumbo, A. V.: Response of marine bacterioplankton to differential filtration and confinement, *Appl. Environ. Microbiol.*, 47, 49–55, <https://doi.org/10.1128/aem.47.1.49-55.1984>, 1984.

270 Halewood, E., Opalk, K., Custals, L., Carey, M., Hansell, D. A., and Carlson, C. A.: Determination of dissolved organic carbon and total dissolved nitrogen in seawater using high temperature combustion analysis, *Front. Mar. Sci.*, 9, 1061646, <https://doi.org/10.3389/fmars.2022.1061646>, 2022.

Han, H., Kim, H. B., Kim, J., Kim, G., Hwang, J., and Nam, S.: Dissolved organic matter in the northwestern Pacific marginal seas: insight into the distribution of its optical properties, *Front. Mar. Sci.*,  
275 10, 1127803, <https://doi.org/10.3389/fmars.2023.1127803>, 2023.

Hyun, J.-H. and Kim, K.-H.: Bacterial abundance and production during the unique spring phytoplankton bloom in the central Yellow Sea, *Mar. Ecol. Prog. Ser.*, 252, 77–88, <https://doi.org/10.3354/meps252077>, 2003.

Hyun, J.-H., Kim, S.-H., Yang, E. J., Choi, A., and Lee, S. H.: Biomass, production, and control of  
280 heterotrophic bacterioplankton during a late phytoplankton bloom in the Amundsen Sea Polynya, Antarctica, *Deep-Sea Res. Pt. II*, 123, 102–112, <https://doi.org/10.1016/j.dsr2.2015.10.001>, 2016.

Hyun, J.-H.: Resource-limited heterotrophic prokaryote production and its potential environmental impact associated with Mn nodule exploitation in the northeast equatorial Pacific, *Microb. Ecol.*, 52, 244–252, <https://doi.org/10.1007/s00248-006-9012-5>, 2006.

- 285 Kim, B., Baek, Y.-J., Han, H., Lee, H., Youn, S.-H., and Hyun, J.-H.: P-limited prokaryotic heterotrophic production and metabolic balance between prokaryotic carbon demand and phytoplankton primary production in summer in the central Yellow Sea, *Ocean Sci. J.*, 60, 14, <https://doi.org/10.1007/s12601-025-00209-x>, 2025.
- Kirchman, D. L., Morán, X. A. G., and Ducklow, H.: Microbial growth in the polar oceans – role of  
290 temperature and potential impact of climate change, *Nat. Rev. Microbiol.*, 7, 451–459, <https://doi.org/10.1038/nrmicro2115>, 2009.
- Nimptsch, J., Woelfl, S., Kronvang, B., Giesecke, R., González, H. E., Caputo, L., Gelbrecht, J., von Tuempling, W., and Graeber, D.: Does filter type and pore size influence spectroscopic analysis of freshwater chromophoric DOM composition?, *Limnologia*, 48, 57–64,  
295 <https://doi.org/10.1016/j.limno.2014.06.003>, 2014.
- Rahav, E., Raveh, O., Hazan, O., Gordon, N., Kress, N., Silverman, J., and Herut, B.: Impact of nutrient enrichment on productivity of coastal water along the SE Mediterranean shore of Israel – a bioassay approach, *Mar. Pollut. Bull.*, 127, 559–567, <https://doi.org/10.1016/j.marpolbul.2018.01.036>, 2018.
- Robinson, C. and Williams, P. J. le B.: Temperature and Antarctic plankton community respiration, *J.*  
300 *Plankton Res.*, 15, 1035–1051, <https://doi.org/10.1093/plankt/15.9.1035>, 1993.
- Saadi, I., Borisover, M., Armon, R., and Laor, Y.: Monitoring of effluent DOM biodegradation using fluorescence, UV and DOC measurements, *Chemosphere*, 63, 530–539, <https://doi.org/10.1016/j.chemosphere.2005.07.075>, 2006.
- Seo, J., Kim, G., Hwang, J., Na, T., Cho, H.-M., and Kim, J.: Measurement of fluorescent dissolved  
305 organic matter in water: methodological considerations and applications, *Biogeosciences*, 22, 4423–4431, <https://doi.org/10.5194/bg-22-4423-2025>, 2025.
- Tsai, A.-Y., Gong, G.-C., Huang, J.-K., and Lin, Y.-C.: Viral and nanoflagellate control of bacterial production in the East China Sea summer 2011, *Estuar. Coast. Shelf Sci.*, 120, 33–41, <https://doi.org/10.1016/j.ecss.2013.01.006>, 2013.

- 310 Vonk, J. E., Tank, S. E., Mann, P. J., Spencer, R. G. M., Treat, C. C., Striegl, R. G., Abbott, B. W., and  
Wickland, K. P.: Biodegradability of dissolved organic carbon in permafrost soils and aquatic systems: a  
meta-analysis, *Biogeosciences*, 12, 6915–6930, <https://doi.org/10.5194/bg-12-6915-2015>, 2015.
- White, P. A., Kalff, J., Rasmussen, J. B., and Gasol, J. M.: The effect of temperature and algal biomass  
on bacterial production and specific growth rate in freshwater and marine habitats, *Microb. Ecol.*, 21, 99–  
315 118, <https://doi.org/10.1007/BF02539147>, 1991.